Journal of Advanced College of Engineering and Management

Comparative Assessment Of Raw And Downscaled CMIP6 Multi-Model Ensembles For Projecting Temperature And Precipitation Dynamics In The Tamor River Basin

[1*]Narayan Shrestha, [2]Devi Prasad Bhattarai
[1,2]*Department of Civil Engineering, Pulchowk Campus, IOE, Tribhuvan University, Nepal*
Corresponding email: [*]nrynshrestha606@gmail.com

DOI: 10.3126/jacem.v12i01.93938

Abstract

This study presents a comparative assessment of raw and downscaled CMIP6 multi-model ensembles for projecting temperature and precipitation dynamics in the Tamor River Basin. Utilizing a six-model ensemble under SSP245 and SSP585, the research quantifies the added value of high-resolution NEX-GDDP data and secondary local bias correction. Results indicate a consistent warming trend, with minimum temperatures rising faster than maximums, narrowing the diurnal range. Under SSP585, the downscaled ensemble projects a +4.22°C temperature increase, surpassing +3.72°C projected by raw GCMs. Similarly, downscaling amplifies the wetting signal, projecting a 54% increase in annual precipitation compared to 46% in raw outputs, with significant intensification during monsoon (JJAS) and post-monsoon (ON). These findings suggest that raw GCMs may underestimate thermal stress and hydrological intensification in complex Himalayan terrains. Overall, downscaled projections provide improved spatial representation and more consistent climate signals, offering a reliable basis for hydroclimatic assessment.

Keywords*—Tamor Basin, CMIP6, NEX-GDDP-CMIP6, Bias Correction, Multi-Model Ensemble, Climate Change Impact*

1. INTRODUCTION

The Hindu Kush Himalayan (HKH) region is one of the most vulnerable hotspots to climate change globally, with studies indicating accelerated warming at high elevations exceeding global averages by 0.06–0.1 °C per decade [1, 2]. This enhanced warming threatens the cryosphere, alters river discharge regimes, and affects the livelihoods of millions relying on climate-sensitive water resources [3].

Effective climate adaptation and water resource management in mountainous regions require robust local-scale climate projections. While Global Climate Models (GCMs) provide the foundation for climate change projections, their coarse resolution (100–250 km) fails to adequately represent the complex topography and climatic gradients typical of Himalayan basins like the Tamor River Basin, resulting in biases especially in precipitation and temperature [4, 5].

Statistical downscaling, particularly Quantile Mapping (QM), is widely used to bridge this scale gap, reducing systematic biases and refining the spatial representation of climate variables from GCM outputs with observational data [6, 7]. Although several studies have evaluated CMIP6 projections for South Asia and parts of the Hindu Kush Himalayan, a systematic comparison between raw and downscaled CMIP6 projections remains limited for eastern Nepal. In high-relief basins such as the Tamor, such evaluations are essential because downscaling can significantly modify projected warming rates, monsoon intensification patterns, and seasonal hydroclimatic dynamics.

The Tamor River supplies nearly 20% of the total flow of the Koshi River, meaning any shifts in temperature or precipitation directly influence the well-being of vast populations in Nepal and India that depend on this water system. Communities rely heavily on the Koshi Basin for water resources, which also holds significant potential for agriculture and large-scale hydropower development within Nepal [8]. These dependencies highlight the importance of understanding basin-scale climate variability and its long-term implications.

However, high-relief Himalayan basins such as Tamor commonly show notable inconsistencies between raw GCM outputs and statistically downscaled climate projections [9]. Most previous studies rely on a single type of projection dataset either raw GCM outputs or pre-processed products and therefore do not systematically evaluate how statistical downscaling influences local climate signal. To address this gap, the present study conducts a comprehensive assessment of future temperature (Tmax and Tmin) and precipitation changes in the Tamor River Basin using a multi-model ensemble of six bias-corrected CMIP6 datasets. The analysis evaluates historical biases, compares raw and downscaled projections, and quantifies future annual and seasonal changes under intermediate (SSP245) and high-emission (SSP585) pathways [10].

The study presents a comparative evaluation of raw and downscaled CMIP6 ensembles specifically for the Tamor River Basin. While earlier studies have utilized raw GCM outputs to assess general trends, they often overlook the inherent limitations of coarse-resolution models in representing the high-relief Himalayan topography. This study advances existing knowledge by quantifying the downscaling signal analyzing how the transition from ~100 km (Raw) to ~25 km (NEX-GDDP) resolution, followed by secondary local bias correction, alters the projected intensity of the monsoon and the narrowing of the diurnal temperature range. By providing this direct comparison, the study clarifies whether high-resolution products are necessary for local-scale adaptation planning in the Koshi sub-basins.

2. STUDY AREA

The Tamor River Basin, located in eastern Nepal, is a major tributary of the Koshi River. It drains a catchment area of approximately 3,900 km^2 and is characterized by extreme topographic diversity (Fig:1), with elevations ranging from around 300 meters in the south to over 7,000 meters in the north, including the Kanchenjunga, the third highest peak. This elevational gradient creates diverse climatic zones from tropical lowland to

snow-dominated environments and results in spatially complex precipitation influenced by both the South Asian monsoon and western disturbances [11, 12].

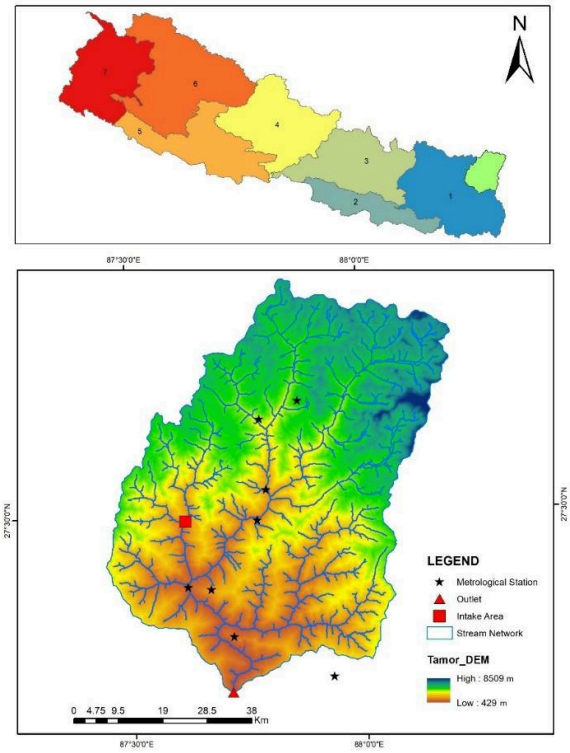

Figure 1: Location map of Study area

The hydrology is dominantly monsoonal (approximately 80% of annual precipitation falls during June-September) with significant contributions from glacier and snowmelt, especially in upper reaches, making it sensitive to seasonal and climate shifts [13]. The basin currently supports agriculture, hydropower projects, and ecosystems vulnerable to climate-induced extremes, such as heavy rainfall-triggered floods and heatwaves [14].

3. DATA AND METHODOLOGY

A. DATASETS

a. General Circulation Model (GCM)

Six CMIP6 models (ACCESS-CM2, CanESM5, CNRM-CM6-1, HadGEM3-GC31-LL, MIROC6, and MPI-ESM1-2-HR) were selected on the basis of their documented skill in simulating South Asian Monsoon dynamics and their frequent use in Himalayan hydro-climatic studies [15, 16, 17]. These models represent a balance of high and medium equilibrium climate sensitivity. To evaluate the effects of downscaling and local calibration, the study compares raw CMIP6 outputs with the Bias-corrected Spatially Disaggregation (BSCD) NEX-GDDP-CMIP6 dataset. Raw GCMs characterize broad scale signals but tend to smooth orographic gradients whereas NEX-GDDP, produced BCSD method,

enhances spatial detail. Furthermore, applying a secondary bias correction to the already-corrected NEX-GDDP data tests the hypothesis that global downscaling products still require local calibration to be reliable for basin-scale application. Projections were analyzed under two emission pathways: SSP245 and SSP585.

b. Climate Data

The Climate data consist of raw CMIP6 GCM (coarse resolution ~1°, 100 km) obtained from the Earth System Grid Federation (ESGF) and the NEX-GDDP-CMIP6 (~0.25°,25 km), which reduces systematic model errors through statistically downscaling [18, 19]. Identical GCMs and SSP scenarios were used for both datasets to isolate the impact of bias correction and downscaling. Analyses were conducted for the historical baseline (1990–2014), mid-century (2041–2070), and late-century (2071–2099) periods. The historical baseline was chosen to maximize overlap with available station records used for bias correction; although slightly shorter than the 30-year standard recommended by the World Meteorological Organization, this period is considered adequate for capturing climatic variability.

c. Bias correction and Multi Model Ensemble (MME) approach

Because residual biases may persist after large-scale BCSD processing, a secondary bias correction using Quantile Mapping (QM) was applied to both raw CMIP6 outputs and the NEX-GDDP product. This correction ensure consistency with local observation from Department of Hydrology and Meteorology (DHM) stations within the complex topography of the Tamor River Basin. Identical correction procedures allow a direct assessment of the "added value" of downscaling versus local calibration.

The bias corrected raw CMIP6 GCM outputs and bias corrected NEX-GDDP-CMIP6 data were each combined into their respective Multi Model Ensemble (MME) means; this MME approach reduces individual model noise and structural uncertainty in the South Asian context [17].

B. VALIDATION OF BIAS CORRECTION

Daily observations from four local stations (IDs: 1403, 1405, 1406, 1420) of the DHM were used as the reference for QM calibration and validation. Missing station values were gap-filled using the APHRODITE–ERA5 merged product [20]. Point observations were interpolated to a basin-scale field using inverse distance weighting (IDW) to create a consistent reference for the historical period. Bias-correction performance was evaluated by comparing raw and bias-corrected model outputs against observations using percent bias (PB), Nash–Sutcliffe efficiency (NSE), and coefficient of determination (R^2) computed from daily basin-averaged Tmax, Tmin, and precipitation. QM substantially reduced systematic biases and RMSE and improved correlations for all variables, with the largest gains for precipitation intensity.

C. METHODOLOGY

The methodological workflow is structured in four main steps:

Step 1: Data Preparation: Raw CMIP6 and NEX-GDDP-CMIP6 downscaled daily datasets for Tmax, Tmin and precipitation were retrieved for the period 1990–2099. Observational data from four DHM stations were quality controlled and gap-filled using APHRODITE-ERA5 to create a reference baseline. These point data were interpolated to a continuous, basin-scale surface using Inverse Distance Weighting (IDW) to create a consistent observational historical period (1990–2014).

Step 2: Secondary Bias Correction: While NEX-GDDP data is pre-processed, a secondary Quantile Mapping (QM) was applied to both Raw and NEX datasets to align them with local station-level topography [6]. This step ensures that the *'added value'* of downscaling is assessed against a consistent local reference.

Step 3: Multi-Model Ensemble (MME): To reduce individual model structural uncertainty, an MME mean was calculated for both datasets across two scenarios (SSP245 and SSP585) for Mid-Future (MF: 2046–2070), and Far-Future (FF: 2071–2099). This helps to reduce individual model noise and provide a more robust consensus signal.

Step 4: Analysis of Projected Climate Change: The projected changes in mean annual temperature and precipitation for the future period relative to the historical period were calculated for both the raw and downscaled datasets under both SSP scenarios. This allowed for a direct comparison of the projected climate signal before and after downscaling.

4. RESULTS

This study utilized a multi-model ensemble (MME) of six bias-corrected CMIP6 Global Climate Models (GCMs), incorporating both raw and statistically downscaled datasets, to project future temperature and precipitation dynamics in the Tamor River Basin. Projections were analyzed under SSP245 (intermediate emissions) and SSP585 (high emissions) scenarios, relative to a 1990–2014 baseline.

A. PROJECTED CHANGE IN ANNUAL TEMPERATURE AND PRECIPITATION

The annual time series of Tmax and Tmin show a clear, persistent rising trend throughout the 21st century. Across all GCMs and the MME, using both raw and downscaled datasets, temperature increases are consistently higher under SSP585 than SSP245, emphasizing the strong dependence of projected warming on emission pathways.

For the bias-corrected raw dataset, projected mean annual Tmax increases range from 0.8°C to 2.1°C under SSP245 and 0.9°C to 3.7°C under SSP585 by the far future. Similarly, Tmin increases range from 0.9°C to 2.1°C under SSP245 and 0.9°C to 4.1°C under SSP585. These magnitudes point to significantly hotter days and notably warmer nights.The bias-corrected downscaled data further reinforce and slightly amplify these

warming trends. Under SSP245, mean annual Tmax increases by 0.9°C to 2.5°C, and under SSP585 by 1.1°C to 4.2°C by FF. For Tmin, increases range from 0.9°C to 2.4°C (SSP245) and 1.0°C to 4.5°C (SSP585).

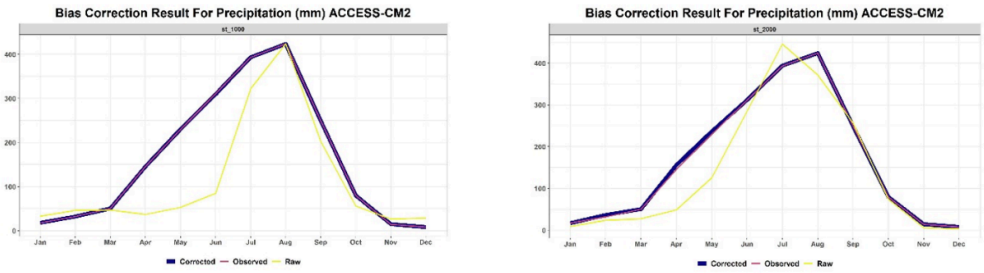

Figure 2: Example of precipitation bias Correction result of Raw and NEX data (ACCESS-CM2)

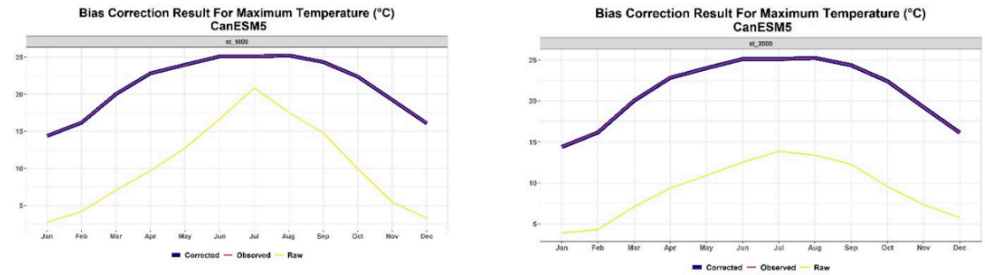

Figure 3: Example of Maximum Temperature bias Correction result of Raw and NEX data (CanESM5)

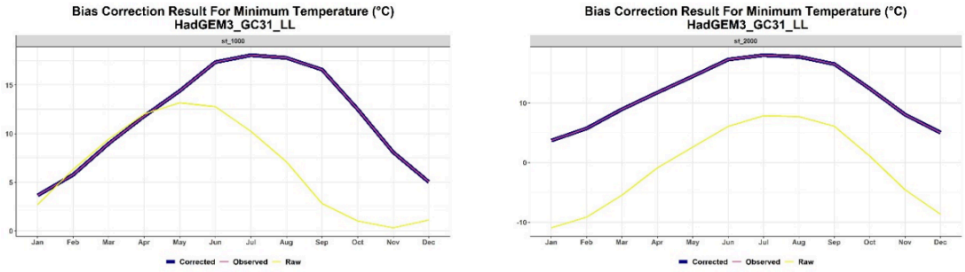

Figure 4: Example of Minimum Temperature bias Correction result of Raw and NEX data (HadGEM3_GC31_LL)

Under SSP585 in the far future, the downscaled ensemble projects a mean annual Tmax increase of +4.22 °C, with an interquartile range (IQR) of 1.64 °C and model projections ranging from 2.74 °C to 5.73 °C, indicating substantial inter-model spread. The corresponding raw ensemble shows a lower mean increase of +3.72 °C (IQR = 1.25 °C, range 2.55–5.21 °C).

Downscaling projection shows fewer inconsistencies compared to raw outputs. For instance, while raw HadGEM3_GC_LL exhibits cooling in certain periods, the downscaled version shows consistent warming throughout, contributing to more coherent ensemble signal.

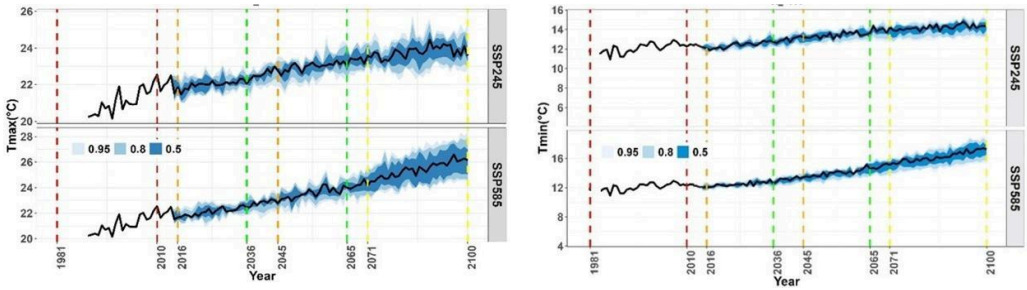

Figure 5: Multi-Model Ensembled of Projected Annual Maximum and Minimum Temperature. The values 0.95, 0.8, and 0.5 represent the 95%, 80%, and 50% confidence intervals, respectively, indicating uncertainty range and spread of ensemble projections.

Table 1: Annual Change in Bias-Corrected Minimum Temperature (Ensemble Mean, °C)

Scenario	Time	Raw Dataset	Downscaled Data
SSP 245	NF	+0.9	+0.9
	MF	+1.5	+1.6
	FF	+2.1	+2.4
SSP 585	NF	+0.9	+1.0
	MF	+1.9	+2.0
	FF	+4.1	+4.5

Table 2: Annual Change in Bias-Corrected Maximum Temperature (Ensemble Mean, °C)

Scenario	Time	Raw Dataset	Downscaled Data
SSP 245	NF	+0.8	+0.9
	MF	+1.3	+1.6
	FF	+2.1	+2.5

SSP 585	NF	+0.9	+1.1
	MF	+1.6	+2.0
	FF	+3.7	+4.2

Precipitation projections exhibit greater variability than temperature. The MME shows that annual precipitation does not follow a simple monotonic increase; rather, it exhibits slight increases or near-stability in the NF period followed by pronounced increases toward the FF, particularly under SSP585. Downscaled datasets tend to amplify these wetting signals. For example, mean annual precipitation increases by +22% (SSP245) and +46% (SSP585) in the raw data by FF, while the bias-corrected downscaled data project increases up to +22% (SSP245) and +54% (SSP585).

For SSP585 in the far future, downscaled annual precipitation increases by an average of +54.8%, with a wide interquartile range of 33.3% and individual model projections spanning from +6.5% to +144.1%. The raw ensemble projects a lower mean increase of +44.3% (IQR = 33.6%), with values ranging from +12.5% to +100.0%, highlighting substantial inter-model uncertainty. The wide ensemble spread suggests considerable uncertainty and the potential for increased hydrological extremes.

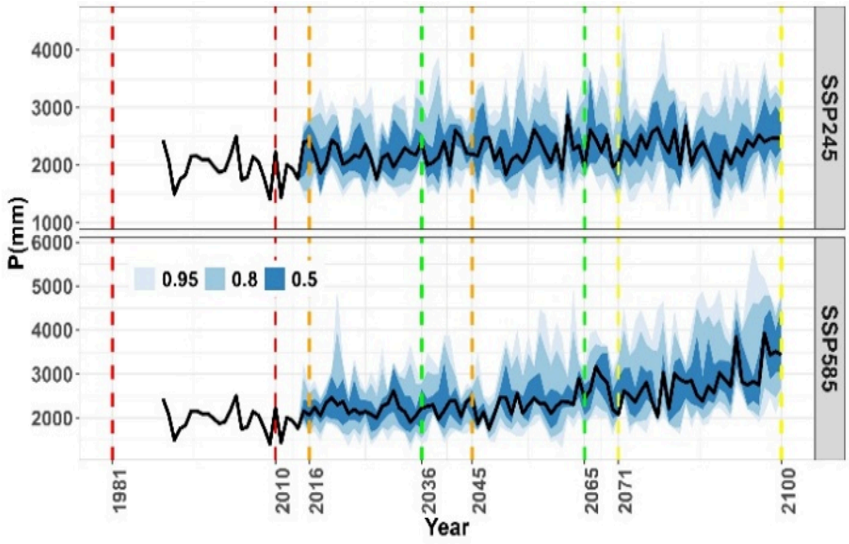

Figure 6: Multi-Model Ensembled of Projected Annual Precipitation. The values 0.95, 0.8, and 0.5 represent the 95%, 80%, and 50% confidence intervals, respectively, indicating uncertainty range and spread of ensemble projections.

Table 3: Annual Change in Bias-Corrected Precipitation (% Change)

Scenario	Time	Raw Dataset	Downscaled Data
SSP 245	NF	+4%	+15%
	MF	+7%	+19%
	FF	+22%	+22%
SSP 585	NF	+3%	+17%
	MF	+6%	+23%
	FF	+46%	+54%

B. PROJECTED CHANGE IN SEASONAL TEMPERATURE AND PRECIPITATION

Seasonal projections highlight important intra-annual shifts that are more relevant for water resources and climate-sensitive sectors. Changes in Tmax, Tmin, and precipitation were examined for winter (DJF), pre-monsoon (MAM), monsoon (JJAS), and autumn (ON).

a. Seasonal Temperature

Projected Tmin increases are strong and persistent across all seasons, with pre-monsoon (MAM) and autumn (ON) exhibiting the largest warming. Under the downscaled SSP585-FF scenario, Tmin increases by +4.8°C in ON, +3.2°C in DJF, +5.5°C in MAM, and +4.4°C in JJAS. These changes imply a substantial narrowing of the diurnal temperature range and warmer cold seasons, influencing snow and glacier dynamics.

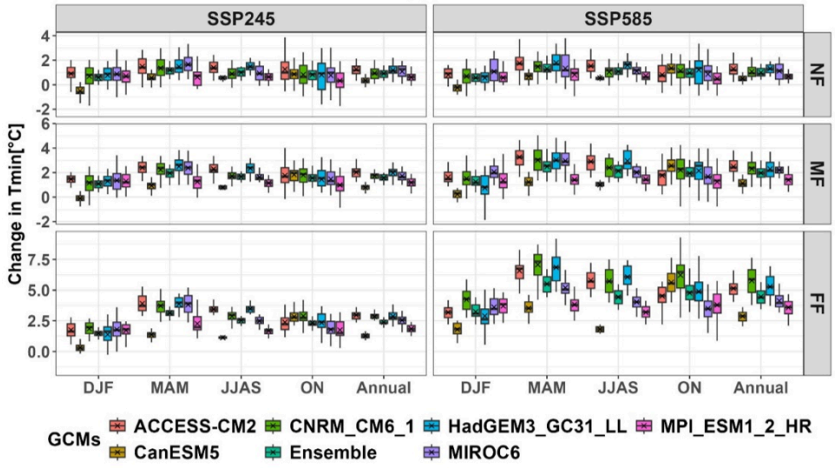

Figure 7: Seasonal changes in Minimum Temperature from Bias Corrected Downscaled Data

Tmax shows consistent warming across seasons, though magnitudes vary. MAM and DJF commonly show the largest Tmax increases in the ensemble. JJAS (summer/monsoon) warming is model-dependent, some GCMs indicate strong JJAS warming while others show moderate changes. Summer (JJAS) warming is pronounced, reaching 3.6°C in raw data and 4.3°C in downscaled data under SSP585-FF; however, inter-model uncertainty is comparatively lower for seasonal temperature, with the downscaled JJAS Tmax ensemble exhibiting an interquartile range of approximately 1.75 °C. Winter (DJF) also shows substantial warming: up to 3.9°C (raw) and 4.4°C (downscaled). MAM and ON show steady, moderate increases across both datasets and scenarios, contributing to longer warm seasons.

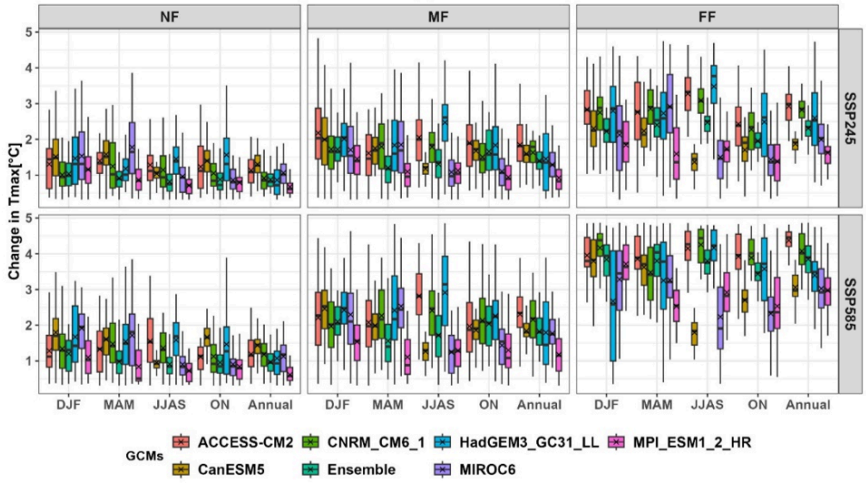

Figure 8: Seasonal changes in Maximum Temperature from Bias Corrected Downscaled Data

Table 4: Seasonal Temperature Changes (Downscaled, Ensemble Mean, °C, FF)

Season	SSP 245 (FF)	SSP 585 (FF)
DJF	+1.5°C	+3.2°C
MAM	+3.2°C	+5.5°C
JJAS	+2.5°C	+4.4°C
ON	+2.3°C	+4.8°C

b. Seasonal Precipitation

Seasonal precipitation shows a more complex and strong seasonal redistribution, with significant increases projected for JJAS and ON. Post-Monsoon (ON) exhibits the most dramatic increases: +37% (SSP245) to +101% (SSP585) change by FF. Monsoon (JJAS) shows a substantial increase +24% (SSP245) to +55% (SSP585) by FF. Under SSP585-FF, downscaled JJAS precipitation increases by an average of

+38.8%, with an interquartile range (IQR) of 31.0% and individual model projections ranging from +5.5% to +132.1%. In contrast, the raw ensemble projects a weaker increase of +16.2% (IQR = 14.9%), with a narrower range of +3.4% to +29.1%. Winter (DJF) and Pre-Monsoon (MAM) show increases in the ensemble mean, the signal is less consistent and subject to higher inter-model variability compared to JJAS and ON.

This pattern suggests an intensification of the rainfall season, with a much wetter monsoon and a significantly enhanced post-monsoon period, potentially altering the hydrological regime of the basin.

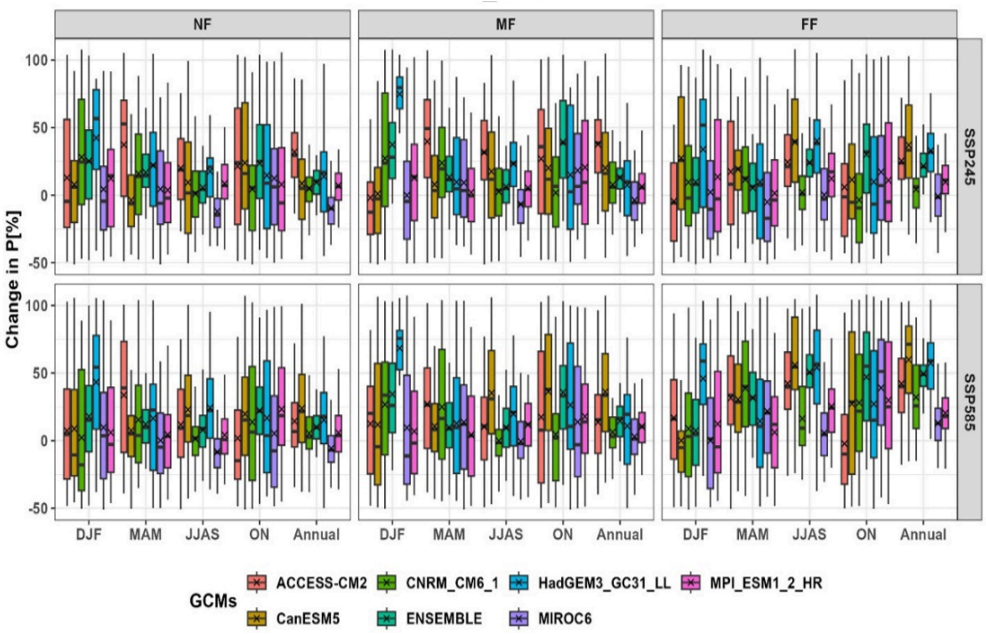

Figure 9: Seasonal changes in Precipitation from Bias Corrected Downscaled Data

Table 5: Seasonal Precipitation Changes (Downscaled, Ensemble Mean, FF)

Season	SSP 245 (FF)	SSP 585 (FF)
DJF	+31%	+31%
MAM	+9%	+41%
JJAS	+24%	+55%
ON	+37%	+101%

Table 6: Ensemble mean and inter-model spread (IQR and min-max) of projected annual and seasonal changes under SSP585 (far-future period)

Variable	Period	Dataset	Mean	IQR	Min-Max
Prec. (%)	Annual	Raw	44.3	33.6	12.5–100.0
Prec. (%)	Annual	Downscaled	54.8	33.3	6.5–144.1
Prec. (%)	JJAS	Raw	16.2	14.9	3.4–29.1
Prec. (%)	JJAS	Downscaled	38.8	31.0	5.5–132.1
Prec. (%)	ON	Raw	115.5	56.1	1.1–519.2
Prec. (%)	ON	Downscaled	52.4	45.6	11.2–167.0
Tmax (◦C)	Annual	Raw	3.7	1.3	2.6–5.2
Tmax (◦C)	Annual	Downscaled	4.2	1.6	2.7–5.7
Tmin (◦C)	Annual	Raw	4.1	1.9	2.0–6.3
Tmin (◦C)	Annual	Downscaled	4.4	1.5	2.6–5.8

5. DISCUSSION

The results show a clear warming trend across the Tamor River Basin, with Tmin increasing slightly faster than Tmax in both raw and downscaled CMIP6 datasets. This pattern persists across all future periods and emission scenarios, indicating a continued narrowing of the diurnal temperature range. Warming magnitudes are consistently higher under SSP585 than SSP245, underscoring the dependence of future temperature increases on emission pathways. Downscaled datasets show slightly stronger warming than raw GCMs, reflecting improved representation of local topography and reduced model bias, as seen in the higher temperature increments of the downscaled MME.

Precipitation projections show greater inter-model variability, yet both raw and downscaled ensembles indicate increasing annual and seasonal rainfall toward mid- and late-century. The strongest and most consistent increases occur during the monsoon (JJAS) and post-monsoon (ON) seasons, with downscaled datasets amplifying these wetting signals particularly under SSP585. Winter and pre-monsoon also show increasing tendencies, though with weaker consistency across models.

The comparison of raw and downscaled outputs reveals systematic differences in both magnitude and consistency of projected changes. Downscaling also enhances the magnitude of projected precipitation change (from +46% in raw to +54% in downscaled by FF), suggesting that raw GCMs may underestimate future rainfall in complex mountain basins. Seasonal amplification is strongest in JJAS and ON, indicating intensified monsoonal influence when regional processes are better resolved. Overall, the findings point to a future of consistent basin-wide warming and substantial increases in monsoon and post-monsoon rainfall, with important implications for water resources, flood risks, and climate-sensitive sectors in the Tamor Basin. It should also be noted that temperature

projections in high-relief basins may be influenced by elevation mismatches between GCM grid cells and actual terrain. Temperature projections in high-relief basins are influenced by elevation mismatches between GCM grid cells and actual terrain. In this study, these effects were reduced by using the high-resolution NEX-GDDP-CMIP6 dataset and applying Quantile Mapping (QM) based on observations from DHM. As station data represent elevation-specific conditions, the bias correction inherently accounts for lapse rate effects, although some residual uncertainties may still remain.

Despite consistent ensemble-mean signals of warming and increased precipitation, particularly during the monsoon and post-monsoon seasons, inter-model spread remains substantial, especially for precipitation. The wide interquartile and full model ranges reflect structural uncertainty in future hydroclimatic projections for the Tamor River Basin, indicating that the magnitude of hydrological impacts may vary considerably across plausible climate trajectories. This underscores the importance of interpreting ensemble-mean projections within the broader envelope of model uncertainty and adopting risk-informed approaches in subsequent hydrological and adaptation assessments

6. CONCLUSION

This study evaluates future projections of Tmax, Tmin, and precipitation in the Tamor River Basin using a multi-model ensemble of bias-corrected CMIP6 GCMs, incorporating both raw and statistically downscaled datasets under SSP245 and SSP585 scenarios. The principal conclusions are:

i. Warming Trend: Downscaling provides a more intense warming signal than raw GCMs, with the downscaled MME projecting a Tmax increase of +4.22 °C vs. +3.72 °C in raw data under SSP585, highlighting that coarse models may underestimate thermal stress in high-altitude zones

ii. Annual Precipitation Rise: The objective of identifying precipitation shifts revealed that downscaled data amplifies the wetting signal (+54% increase) compared to raw data (+46%), suggesting that improved spatial resolution better captures the intensification of the hydrological cycle in the monsoon and post-monsoon seasons

iii. Seasonal Rainfall Shift: Monsoon (JJAS) and post-monsoon (ON) rainfall intensify markedly, indicating a more concentrated rainfall season and higher flood risk.

iv. Role of Downscaling: The downscaled projections show notable differences from the raw GCM outputs, including relatively stronger precipitation intensification signals, particularly during the monsoon and post-monsoon seasons and improved spatial resolution that better represents the basin's complex topography, thereby supporting a more reliable hydroclimatic assessment

The downscaled multi-model ensemble (MME) therefore provides a more robust foundation for assessing future climate risks by reducing systematic model biases. Overall, the Tamor River Basin is expected to undergo substantial warming and a progressively intensified hydrological cycle, with significant implications for water availability,

agriculture, ecosystems, and disaster risk. While ensemble-mean projections indicate robust warming and intensified precipitation, particularly during the monsoon and post-monsoon seasons, the magnitude of future hydroclimatic impacts remains uncertain due to inter-model variability, highlighting the importance of risk-informed interpretation. The differences between SSP245 and SSP585 highlight the importance of global mitigation efforts, while the projected changes underscore the need for strengthened regional adaptation strategies. The projections generated in this study provide a valuable basis for future hydrological modeling and climate-impact assessments in the basin.

ACKNOWLEDGMENTS

For all of their tremendous support and direction throughout the entire study project, the authors would like to sincerely thank the Department of Applied Science and Chemical Engineering, Pulchowk Campus, IOE, TU.

REFERENCES

[1] Raymond S. Bradley, Mathias Vuille, H. F. Diaz, and Walter Vergara. Threats to water supplies in the tropical andes. Science, 312(5781):1755–1756, 2006.

[2] Anil B. Shrestha et al. Climate change in nepal and its impact on himalayan glaciers. Journal of Mountain Science, 9(6):650–661, 2012.

[3] Tobias Bolch et al. Status and change of the cryosphere in the extended hindu kush himalaya region. In P. Wester, A. Mishra, A. Mukherji, and A. B. Shrestha, editors, The Hindu Kush Himalaya Assessment, pages 187–214. Springer, Cham, 2019.

[4] E. Palazzi, J. von Hardenberg, and A. Provenzale. Precipitation in the hindu–kush karakoram himalaya: Observations and future scenarios. Journal of Geophysical Research: Atmospheres, 118:85–100, 2013.

[5] Walter W. Immerzeel, Ludovicus P. H. Van Beek, and Marc F. P. Bierkens. Climate change will affect the asian water towers. Science, 328(5984):1382–1385, 2010.

[6] Lukas Gudmundsson, John B. Bremnes, Jan E. Haugen, and Torill Engen-Skaugen. Technical note: Downscaling rcm precipitation to the station scale using statistical transformations – a comparison of methods. Hydrology and Earth System Sciences, 16(9):3383–3390, 09 2012.

[7] Alex J. Cannon, Stephen R. Sobie, and Trevor Q. Murdock. Bias correction of gcm precipitation by quantile mapping: How well do methods preserve changes in quantiles and extremes Journal of Climate, 28(17):6938–6959, 2015.

[8] S. Nepal, W.-A. Flügel, and A. B. Shrestha. Upstream–downstream linkages of hydrological processes in the himalayan region. Ecological Processes, 3:19, 2014.

[9] V. Mishra. Climatic uncertainty in himalayan water towers. Journal of Geophysical Research: Atmospheres, 2015.

[10] Brian C. O'Neill et al. The scenario model intercomparison project (scenariomip) for cmip6. Geoscientific Model Development, 9:3461–3482, 2016.

[11] Bodo Bookhagen and Douglas W. Burbank. Topography, relief, and trmm-derived rainfall variations along the himalaya. Geophysical Research Letters, 33(8):L08405, 2006.

[12] D. R. Archer and H. J. Fowler. Spatial and temporal variations in precipitation in the upper indus basin, global teleconnections and hydrological implications. Hydrology and Earth System Sciences, 8(1):47–61, 02 2004.

[13] J. M. Shea, G. S. Hamilton, and S. Rupper. A comparative high-altitude meteorological analysis from central and eastern nepal. Arctic, Antarctic, and Alpine Research, 47(3):739–750, 2015.

[14] ICIMOD. Himalaya climate outlook. Technical report, ICIMOD, 2020. ICIMOD Report.

[15] Vimal Mishra, Udit Bhatia, and Atul D. Tiwari. Bias- corrected climate projections from cmip6 for south asia. Scientific Data, 7(1):338, 2020.

[16] Markus Lamichhane, Suraj Phuyal, Dipesh Neupane, and et al. Assessing climate change impacts in the karnali river basin using a cmip6 multi-model ensemble and swat. Sustainability, 16(8):3262, 2024.

[17] S. R. Subedi, M. Lamichhane, S. Dhungana, B. Chalise, S. Bhattarai, U. Chaulagain, and R. Khatiwada. Assessing the impact of climate change on streamflow in the tamor river basin, nepal: An analysis using swat and cmip6 scenarios. Discover Civil Engineering, 3:14, 2024.

[18] B. Thrasher et al. Bias correction and statistical downscaling for cmip6 climate projections. Earth System Science Data, 14(9):4017–4039, 09 2022.

[19] NASA. Nasa earth exchange global daily downscaled climate projections (nex-gddp-cmip6). https://www.nccs.nasa.gov/services/ data-collections/land-based-products/ nex-gddp, 2021. NASA Center for Climate Simulation.

[20] Piyush Dahal, Nicky Shree Shrestha, Madan L. Shrestha, Nir Y. Krakauer, Jeeban Panthi, Soni M. Pradhanang, Ajay Jha, and Tarendra Lakhankar. Drought risk assessment in central nepal: temporal and spatial analysis. Natural Hazards, 80:1913–1932, 2016.

[21] Siraj Beshir. Climate change projections using cmip6 gcms and downscaling approaches in the upper wabe shebele basin, ethiopia. Scientific Reports, 15:39521, 2025.